Journal of Organometallic Chemistry 745-746 (2013) 347–355

Contents lists available at ScienceDirect

Journal of Organometallic Chemistry

journal homepage: www.elsevier.com/locate/jorganchem

Formation of phosphorus heterocycles using a cationic electrophilic phosphinidene complex

Kandasamy Vaheesar, Colin M. Kuntz, Brian T. Sterenberg*

Department of Chemistry and Biochemistry, University of Regina, 3737 Wascana Parkway, Regina, Saskatchewan, Canada S4S 0A2

ARTICLE INFO

Article history:
Received 20 June 2013
Received in revised form
24 July 2013
Accepted 30 July 2013

Keywords:
Phosphinidene
Cycloaddition
Phosphorus heterocycle
Metal-mediated synthesis

ABSTRACT

The electrophilic terminal aminophosphinidene complex $[CpFe(CO)_2P\{N\text{-}i\text{-}Pr_2\}][X]$ (Cp = cyclopentadienyl, *i*-Pr = isopropyl, *X* = $AlCl_4$ or $NaBPh_4$), generated from $[CpFe(CO)_2\{P(Cl)N\text{-}i\text{-}Pr_2\}]$ by chloride abstraction, reacts with alkynes and alkenes via (1 + 2) cycloaddition to form phosphirenes and phosphiranes respectively. Conjugated alkenes react with $[CpFe(CO)_2P\{N\text{-}i\text{-}Pr_2\}]^+$ to form phosphirane intermediates, which then rearrange to 3-phospholenes. The phosphinidene complex reacts with benzylideneacetone to give an oxo-3-phospholene complex. Azobenzene reacts with $[CpFe(CO)_2P\{N\text{-}i\text{-}Pr_2\}]^+$ to form a benzodiazophosphole via C–H activation. Addition of HCl or $HBF_4{\cdot}Et_2O$ to the iron diphenylphosphirene complex and iron benzodiazophosphole complex results in P–N bond cleavage, yielding the respective chlorophosphorus heterocyclic complexes. The heterocycles can be removed from the metal complexes to make metal free phosphorus heterocycles by addition of trimethyl- or triethylphosphine.

1. Introduction

Transition metal terminal phosphinidene complexes can be considered analogous to metal carbene complexes, and like carbenes, their reactivity ranges from nucleophilic to electrophilic extremes [1–3]. The first electrophilic terminal complexes were the transient species $[W(CO)_5PR]$, generated *in situ* by thermal decomposition of precursor 7-phosphanorbornadiene complexes [4]. Their reactivity has been well studied using trapping reactions with a variety of reagents [5–7]. These trapping reactions, in conjunction with computational studies [1,2,8–11], provide a clear understanding of the chemistry of transient electrophilic phosphinidene complexes. Their characteristic reactions include bond activation, nucleophilic addition, and cycloaddition reactions to form P-heterocycles. Stable electrophilic terminal phosphinidene complexes of molybdenum and tungsten were first reported in 2001 [12]. Since then a wide range of stable electrophilic terminal phosphinidene complexes have been synthesized [13–16]. The reactivity of stable, cationic phosphinidene complexes has not been as well studied as that of the neutral transient species, but examples of nucleophilic addition [17], bond activation [18], and cycloaddition reactions [13,16] have been described.

We were interested in carrying out a more comprehensive study of cycloaddition reactions of a stable, cationic phosphinidene complex. The first objective was to see if the typical reactivity of these complexes differs in any significant way from that of the neutral, transient complexes. The second goal was to see if these reactions can be developed into a useful synthetic route to functional P heterocycles for synthetic applications such as ligand synthesis. With the second goal in mind, we chose $[CpFe(CO)_2\{PN\text{-}i\text{-}Pr_2\}]^+$ [15] as our metal complex, because it is relatively easy to synthesis and inexpensive enough to be useful for stoichiometric synthesis, and because *i*-Pr_2N group is potentially cleavable, providing a route to further functionalization.

2. Results and discussion

2.1. Cycloaddition reactions

The electrophilic terminal aminophosphinidene complex $[CpFe(CO)_2\{PN\text{-}i\text{-}Pr_2\}][AlCl_4]$ (**2a**) is readily formed by abstraction of chloride from the chloroaminophosphido complex $[CpFe(CO)_2\{P(Cl)N\text{-}i\text{-}Pr_2\}]$ (**1**) using $AlCl_3$. The chloride can also be abstracted from **1** using $NaBPh_4$, leading to $[CpFe(CO)_2\{PN\text{-}i\text{-}Pr_2\}][BPh_4]$ (**2b**), giving us a choice of counterion. Reactions of **2** can be carried out either with isolated aminophosphinidene complex or *in situ*. Because the aminophosphinidene is very sensitive, we typically generate it *in situ* and react it with a substrate without isolating it.

* Corresponding author. Tel.: +1 306 585 4106.
E-mail address: brian.sterenberg@uregina.ca (B.T. Sterenberg).

0022-328X/$ – see front matter © 2013 Elsevier B.V. All rights reserved.
http://dx.doi.org/10.1016/j.jorganchem.2013.07.076

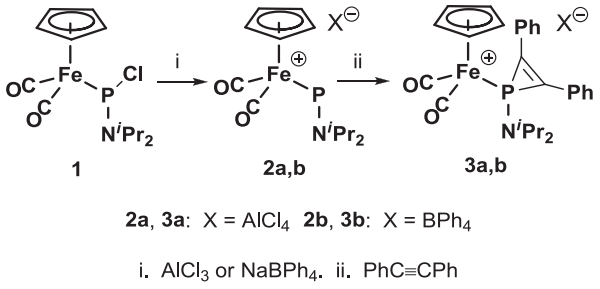

Scheme 1.

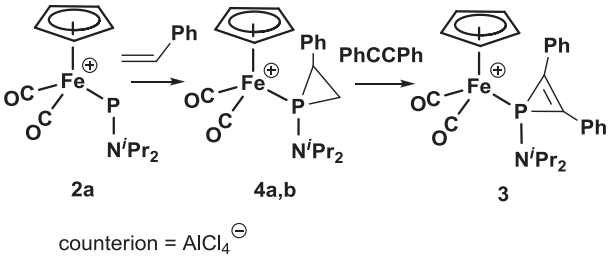

Scheme 2.

Reaction of the aminophosphinidene complex **2** with diphenylacetylene results in a (1 + 2) cycloaddition, leading to the aminophosphirene complex **3** (Scheme 1). The ^{31}P NMR spectrum of **3** shows a characteristic high field shift at δ −69.7. High field chemical shifts in ^{31}P NMR spectrum are characteristic of phosphorus in three-membered rings [19–21]. The infrared spectrum shows carbonyl stretching frequencies at 2059 and 2016 cm^{-1}. Complex **3b** (BPh_4^- counterion) has been structurally characterized (Fig. 1). The cation consists of $CpFe(CO)_2$ fragment coordinated by an aminophosphirene ring. The di-isopropylamino group is oriented away from the Cp ring. The P–N bond distance is 1.672(2) Å, which is consistent with a nitrogen–phosphorus single bond. Bond distances and angles within the three-membered ring are consistent with those of previously characterized phosphirenes [4,13,22,23].

Compound **2** reacts with styrene to form the phosphirane complex $[CpFe(CO)_2\{P(N\text{-}i\text{-}Pr_2)CH(Ph)CH_2\}][AlCl_4]$ (**4a**, **b**) (Scheme 2). However, **2** does not react with the more sterically crowded stilbene, even at 100 °C. The ^{31}P NMR spectrum of **4** shows two peaks at δ −52.0 (81%) and −53.8 (19%) that result from two diastereoisomers. Compound **4a** has been structurally characterized and an ORTEP diagram is shown in Fig. 2. In the diastereomer crystallized, the $CpFe(CO)_2$ fragment and the phenyl group are on the same side of PC_2 ring and the amino group is on the opposite side. The Ph group is presumably on the opposite side to the $CpFe(CO)_2$ fragment in the other diastereomer.

The styrene in **4** can be readily displaced by an alkyne to form aminophosphirene **3**, showing that the phosphinidene has a greater affinity for alkynes than alkenes. This reaction also suggests that **4** is in equilibrium with its components, phosphinidene and styrene. This equilibrium was confirmed by dissolution of crystals of **4** in CD_2Cl_2, which resulted in the formation of a solution containing both **2** and **4**. Addition of excess styrene drives the equilibrium toward **4**.

Reaction of **2** with isoprene (2-methyl-1,3-butadiene) led to the 2-phospholene complex **6**. The ^{1}H NMR spectrum of **6** shows the expected resonances for the 3-phospholene alkenyl (δ 3.98), methylene (δ 3.38 and 2.81), and methyl (δ 1.86) protons. Direct monitoring of the reaction solution immediately after addition of isoprene revealed the presence of two additional intermediates that eventually convert to **6**. If the reaction is carried out at 0 °C, the intermediates can be formed as the major components. The ^{31}P chemical shifts of δ −49.7 and −51.9 are consistent with their formulation as vinylphosphiranes **5a** and **5b** (26:1), indicating that **6** is formed via (1 + 2) addition followed by ring expansion (Scheme 3).

Because the isoprene product **6** was persistently non-crystalline, compound **2** was also reacted with 1,4-diphenyl-1,3-butadiene to form the analogous 3-phospholene complex **7** (Scheme 3). In this case the reaction is much slower, requiring 8 h at 60 °C. Because of the higher temperatures, no phosphirane intermediates could be detected. This reactivity contrasts with that of the neutral transient phosphinidene $[W(CO)_5PPh]$, which reacts with 1,4-diphenyl-1,3-butadiene to form a vinylphosphirane, but does not give the corresponding phospholene complex [24]. The steric size of the metal complex may be controlling regioselectivity, in that the smaller $CpFe(CO)_2$ fragment allows a rearrangement to the 3-phospholene, which the larger $W(CO)_5$ fragment prevents. Compound **7** has been structurally characterized (Fig. 3). The cation consists of $CpFe(CO)_2$ fragment coordinated by a phospholene ring. The phospholene ring is a planar. The phenyl groups and the $CpFe(CO)_2$ fragment are

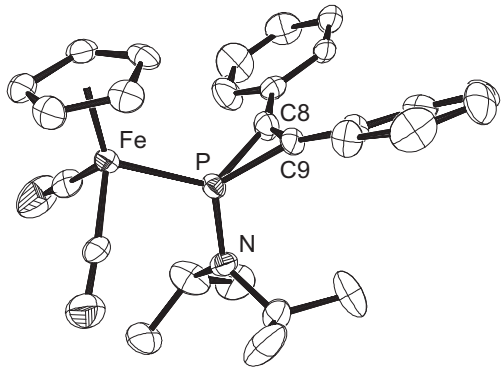

Fig. 1. ORTEP diagram showing the structure of $[CpFe(CO)_2\{P(N\text{-}i\text{-}Pr_2)C(Ph)C(Ph)\}][BPh_4]$ (**3b**). Thermal ellipsoids are shown at the 50% level. Hydrogen atoms and the BPh_4^- counterion have been omitted. Selected distances (Å) and angles (deg): Fe–P = 2.2368(7), P–N = 1.672(2), P–C8 = 1.780(2), P–C9 = 1.780(2), C8–C9 = 1.332(3), C8–P–C9 = 43.9(1), P–C8–C9 = 68.0(1), P–C9–C8 = 68.0(1).

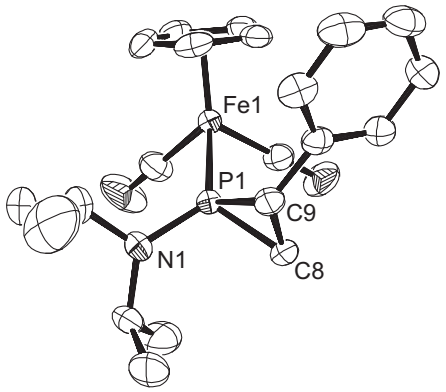

Fig. 2. ORTEP diagram showing the structure of $[CpFe(CO)_2\{P(N\text{-}i\text{-}Pr_2)CH(Ph)CH_2\}][AlCl_4]$ (**4a**). Thermal ellipsoids are shown at the 50% level. Hydrogen atoms and the $AlCl_4^-$ counterion have been omitted. Selected distances (Å) and angles (deg): Fe–P = 2.2272(6), P–N = 1.649(2), P–C8 = 1.800(2), P–C9 = 1.850(2), C9–P–C8 = 49.3(1), P–C9–C8 = 67.1(1), P–C8–C9 = 63.7(1).

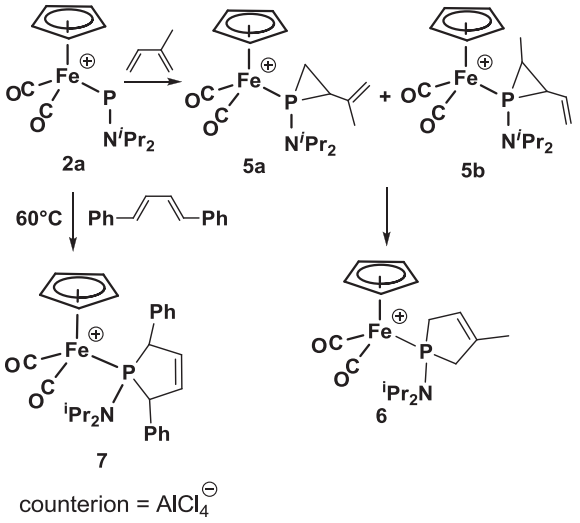

Scheme 3.

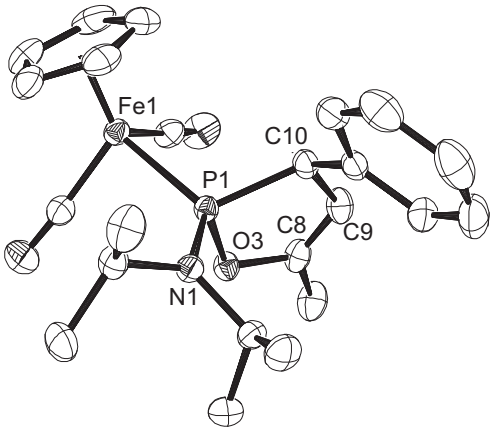

Fig. 4. ORTEP diagram showing the structure of **8**. Thermal ellipsoids are shown at the 50% level. Hydrogen atoms and the $AlCl_4^-$ counterion have been omitted. Selected distances (Å) and angles (deg): Fe–P = 2.2129(5), P–N = 1.643(1), P–O3 = 1.650(1), P–C10 = 1.883(1), O3–C8 = 1.400(2), C10–C9 = 1.505(2), C9–C8 = 1.320(3), C10–P–O3 = 94.41(7), P–O3–C8 = 112.3(1), O3–C8–C9 = 116.1(1), C8–C9–C10 = 116.1(2), C9–C10–P = 101.1(1).

directed to one face of the ring, and the amino group is directed to the other face of the ring. This arrangement allows the metal fragment to sit within a pocket formed by the two phenyl rings. There is no evidence for the formation of other isomers with *trans* phenyl groups, or with *cis* phenyl groups on the *i*-Pr_2N side of the ring.

Reaction of **2** with benzylideneacetone (4-Phenyl-3-buten-2-one) leads to (1 + 4) addition to form the oxo-3-phospholene complex **8** as the sole product (Scheme 4). The ^{31}P NMR spectrum of **8** shows a singlet δ 198.8. In addition to the expected Cp, *i*-Pr, and phenyl peaks, the ^1H spectrum shows a doublet at δ 4.32 (J_{HP} = 27 Hz) for the CH α to P, a broad multiplet at δ 5.49 for the alkenyl hydrogen, and a singlet at δ 2.15 for the ring methyl group. Compound **8** has been structurally characterized and an ORTEP diagram is shown in Fig. 4. The cation consists of $CpFe(CO)_2$ fragment coordinated by an oxo-3-phospholene ring. The oxo-3-phospholene ring is a planar. The amino group and the phenyl group are directed to one face of the ring, and the $CpFe(CO)_2$ fragment is directed to the other face of the ring.

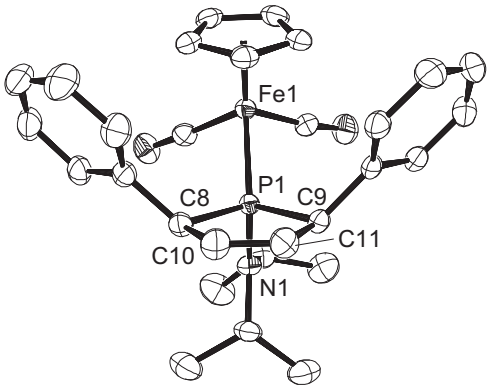

Fig. 3. ORTEP diagram showing the structure of [$CpFe(CO)_2${P(N-*i*-Pr_2)(CH(Ph)-CH=CHCH(Ph))}][$AlCl_4$] (**7**). Thermal ellipsoids are shown at the 50% level. Hydrogen atoms and the $AlCl_4^-$ counterion have been omitted. Selected distances (Å) and angles (deg): Fe–P = 2.2570(9), P–N = 1.681(3), P–C8 = 1.885(3), P–C9 = 1.896(3), C8–C10 = 1.497(4), C9–C11 = 1.488(5), C10–C11 = 1.321(5), C8–P–C9 = 93.9(1), P–C9–C11 = 103.8(2), C9–C11–C10 = 119.7(3), C11–C10–C8 = 118.0(3), C10–C8–P = 104.6(2).

Reaction of **2** with azobenzene leads to a benzodiazophosphole in a reaction that involves ortho C–H activation and proton transfer to N (Scheme 5). This reactivity is the same as that reported for stable cationic rhenium and cobalt phosphinidenes [16], but contrasts with that of neutral transient tungsten phosphinidenes, which simply insert into an ortho C–H bond [25]. Compound **10** was characterized spectroscopically, and the spectral data are consistent with the published data for rhenium and cobalt benzodiazo–phosphole complexes. Notably, the N–H peak appears at δ 7.39. Compound **10** has been structurally characterized, and an ORTEP diagram of the cation is shown in Fig. 5. The structure consists of a $CpFe(CO)_2$ unit coordinated by the benzodiazophosphole ring. The ligand is oriented such that the amino group is directed away from the Cp ring.

2.2. P–N bond cleavage

Part of the reason for choosing an aminophosphinidene as our starting point is the potential cleavability of the P–N bond. In

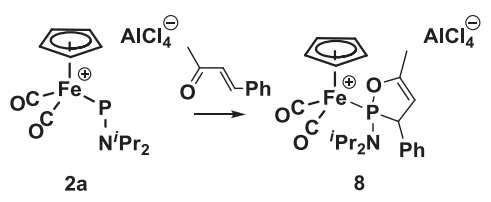

Scheme 4.

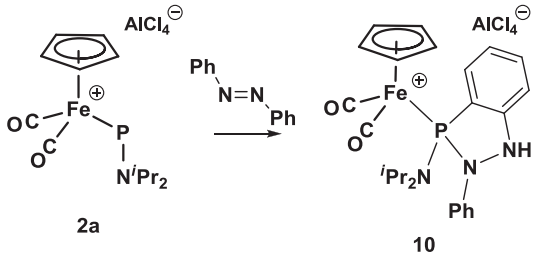

Scheme 5.

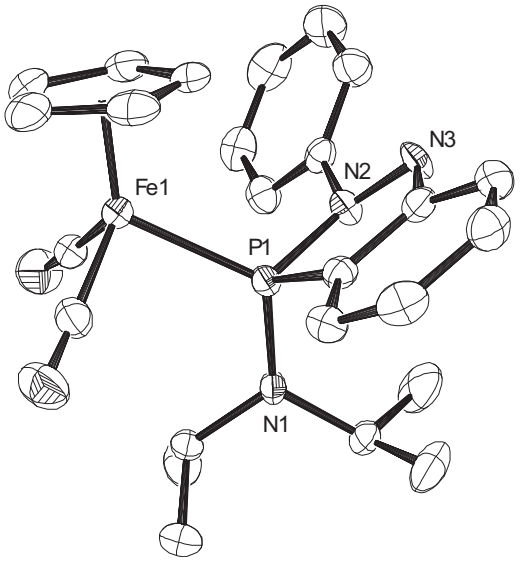

Fig. 5. ORTEP diagram showing the structure of **10**. Thermal ellipsoids are shown at the 50% level. Hydrogen atoms and the $AlCl_4^-$ counterion have been omitted. Selected distances (Å) and angles (deg): Fe–P = 2.2347(9), P–N1 = 1.652(2), P–N2 = 1.716(2), P–C14 = 1.796(3), N2–N3 = 1.428(3), N3–C15 = 1.412(4), C14–C15 = 1.375(4), N1–P–C14 = 112.2(1), N2–P–C14 = 89.9(1), N3–N2–P = 113.6(2), C15–N3–N2 = 109.4(2), C15–C14–P = 110.6(2), C14–C15–N3 = 115.1(3).

particular, conversion to a P–Cl will lead to a useful substrate for further elaboration. It is also potentially useful to cleave the P–N bond while the P-heterocycle is coordinated to the metal fragment, which serves as an effective protecting group for the phosphorus lone pair.

Reaction of the aminodiphenylphosphirene complex **3** with $HCl_{(g)}$ yields the chlorodiphenylphosphirene complex **11** (Scheme 6). This reaction is slow, requiring 8 h to complete amine cleavage. The P–N cleavage reaction can also be carried using $HBF_4{\cdot}Et_2O$. Here the $AlCl_4^-$ counterion provides the Cl^- nucleophile. Separation of the chlorodiphenylphosphirene complex **11** from the side product $[H_2N\text{-}i\text{-}Pr_2]^+ X^-$ ($X^- = AlCl_4^-$, BPh_4^-, BF_4^-) is difficult because both are salts, and extraction of the desired product with a non-polar solvent or selective precipitation is impossible. Column chromatography was not possible on the cationic complexes. Compound **11** was eventually purified by crystallization and manual separation. The difficult separation severely limits the utility of this reaction.

The ^{31}P NMR spectrum of **11** shows a characteristic high field shift at δ −52.0, confirming the retention of phosphirene ring. The ^1H NMR spectrum shows only multiplets at δ 7.93–7.73 for phenyl rings and a singlet at δ 4.89 for the cyclopentadienyl ligand. Peaks for isopropyl groups were not observed, confirming that the N-*i*-Pr_2 group has been removed. The molecular ion in the electrospray mass spectrum shows the expected mass and the characteristic isotope pattern for a Cl atom (m/z = 421, 423), confirming the formula and the presence of chlorine. The infrared spectrum shows carbonyl stretching frequencies at 2077 and 2038 cm^{-1}. When the amine group is substituted by electronegative chlorine atom, the carbonyl stretches shift to higher frequencies, indicating that the chlorophosphirene is a weaker donor than the aminophosphirene. For comparison, compound **3** shows carbonyl stretching frequencies at 2059 and 2016 cm^{-1}.

Reaction of the iron aminobenzodiazophosphole complex **10** with $HBF_4{\cdot}Et_2O$ yields chlorobenzodiazophosphole complex **12** (Scheme 7). This reaction is also slow, and the $AlCl_4^-$ counterion provides the Cl^- nucleophile. Here again, the ^1H NMR confirms the

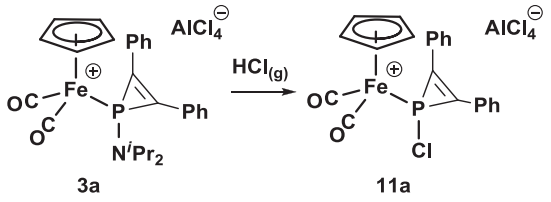

Scheme 6.

complete removal of amino group and the mass spectrum confirm the presence of chlorine atom (m/z = 425, 427).

Attempts to cleave the P–N bond of phosphirane complex **4** by acid addition resulted in loss of styrene and formation of secondary chloroaminophosphine complex **13** (Scheme 8). The ^{31}P NMR spectrum (^1H coupled) of **13** shows a doublet at δ 104.1 with a ^1J(HP)= 473 Hz, indicating a direct P–H bond. The ^1H NMR spectrum shows a peak at δ 8.81 with a large coupling constant that matches that in ^{31}P NMR spectrum. Compound **13** can be independently synthesized by protonation of **1**. The 2-phospholene complexes **6** and **7**, and oxo-phospholene complex **8** showed no evidence of P–N cleavage under prolonged exposure to $HCl_{(g)}$ or $HBF_4{\cdot}Et_2O$.

2.3. Decomplexation

After the formation of phosphorus heterocyclic complexes using the phosphinidene complex, the metal fragment can be removed to isolate the metal free phosphorus heterocycles. We have found that the simplest method is displacement of the P-heterocycle with PMe_3 or PEt_3, leading to the cationic metal complexes $[CpFe(CO)_2PR_3]^+$ (**14**), which are readily separated from the neutral P-heterocycle.

Reaction of diphenylphosphirene complex **3** with PMe_3 yields complex **14** and the free aminophosphorus heterocycle **15** (Scheme 9). The ^{31}P NMR spectrum of **15** shows a singlet at δ −127.7 and ^1H NMR spectrum shows the expected peaks for the phenyl group and the isopropyl groups. The metal complex **14** shows a ^{31}P chemical shift at δ 33.6 and CO stretches at 2052 and 2010 cm^{-1}, comparable to those of known $[CpFe(CO)_2(PR_3)]^+$ complexes [26–28]. The identity of **14** was also confirmed by X-ray crystallography (see Supporting information).

Similar reactions of phospholene complexes **7** and **8** with PMe_3 or PEt_3 give free phospholenes **16** and **17** (Scheme 10). Displacement of the phospholenes is slower, but can be accelerated with heat. The ^{31}P NMR spectrum of **16** shows a singlet at δ 91.4, while the ^1H NMR spectrum shows doublets at δ 5.89 and 5.70 for the phospholene ring protons, as well as the expected phenyl and isopropyl resonances. The ^{31}P NMR spectrum of **17** shows a singlet at δ 137.0. In the ^1H NMR spectrum, the alkenyl hydrogen appears as a doublet of doublets of quartets at δ 5.07. A broad doublet at δ 4.33 with phosphorus coupling of 32 Hz is assigned as the oxo-3-

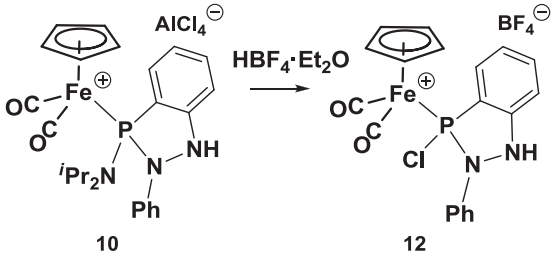

Scheme 7.

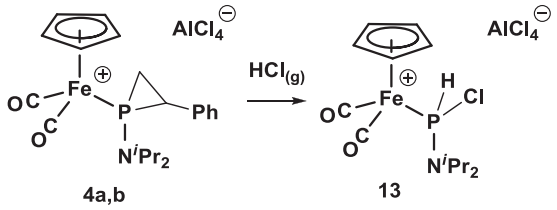

Scheme 8.

phospholene methyne proton. The isopropyl methyne and methyl protons appear at δ 3.00 and 1.11 as broad peaks. Reaction of aminobenzodiazophosphole complex **10** with trimethylphosphine yields the expected iron phosphine complex **14**, but the free aminobenzodiazophosphole decomposes during workup.

Reaction of phosphirane complex **4** with phosphines does not result in decomplexation. Instead styrene is displaced to form phosphine coordinated phosphinidene complexes (Scheme 11). Compound **18**, the product that results from reaction of **4** with triethylphosphine, has been fully characterized. The ^{31}P NMR spectrum shows doublets at δ 90.7 and 11.3 with a common coupling constant ^{1}J(PP) = 517 Hz, confirming the direct P–P bond. Compound **18** can also be formed by reaction of PEt_3 with **2**.

Decomplexation of the chlorophosphirene complex **11c** occurs simply upon dissolution in THF. When compound **11c** (BF_4^- counterion) was stirred in THF for 30 min the peak at δ −52.0 in the ^{31}P NMR spectrum disappeared and a new peak at δ −80.7 was observed. After pentane extraction the two products were separated using chromatography on a silica gel column with dichloromethane eluent and were shown to be the chlorophosphirene **19** and [CpFe(CO)$_2$F] (**20**) (Scheme 12). The spectra of **19** [29] and **20** [30] are consistent with the published data.

3. Conclusions

The cationic iron phosphinidene complex under examination here undergoes cycloaddition reactions with a wide range of unsaturated substrates, and primarily shows the typical reactivity expected for electrophilic phosphinidene complexes. Attempts to convert the amino group to a chloro group in the metal coordinated heterocycles showed limited success. The conversion is only possible for phosphirene and benzodiazophosphole complexes, and even when the reaction is successful, separation and isolation of the products tends to be difficult. Here, the cationic nature of the metal complex is a distinct disadvantage. From this we conclude that chlorination is best carried out after decomplexation. Chlorination reactions of amino substituted P-heterocycles are well described in the literature [31–35]. In decomplexation reactions, the cation metal complex is advantageous because it allows separation of neutral P-heterocycles from the metal complex via simple extraction.

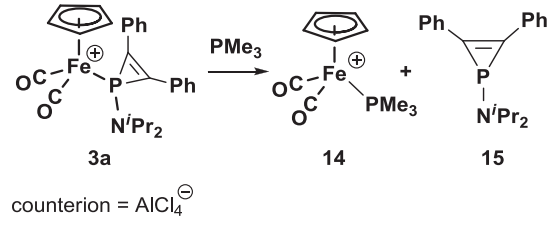

Scheme 9.

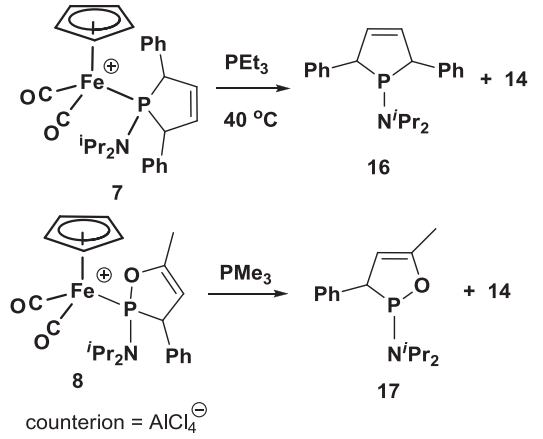

Scheme 10.

4. Experimental section

4.1. General comments

All procedures were carried out under a nitrogen atmosphere using standard Schlenk techniques or in an inert atmosphere glovebox. Pentane was distilled from $NaK_{2.8}$/benzophenone, THF was distilled from Na/benzophenone, and dichloromethane and hexane were purified using solvent purification columns containing alumina (dichloromethane) or alumina and copper catalyst (hexane). Deuterated chloroform was distilled from P_2O_5. The NMR spectra were recorded in $CDCl_3$, CD_2Cl_2 or DMSO-d^6 using a Varian Mercury 300 MHz spectrometer at 300.179 MHz (^{1}H), 121.515 MHz (^{31}P{^{1}H}), 75.479 MHz (^{13}C{^{1}H}) or 282.449 (^{19}F{^{1}H}). Infrared spectra were recorded in $CDCl_3$ or CH_2Cl_2 solution using a Digilab FTS-3000 spectrometer. Mass spectra of metal complexes were obtained using a Finnigan–Matt TSQ-700 mass spectrometer equipped with electrospray ionization and a Harvard syringe pump. The compound [CpFe(CO)$_2${P(Cl)N-*i*-Pr$_2$}] (**1**) was synthesized using the published procedure [15]. Compound **2** was prepared using modifications of the published procedure [15] as described below.

4.2. Cycloaddition reactions

4.2.1. [CpFe(CO)$_2${P(N-*i*-Pr$_2$)(C(Ph)C(Ph)}][AlCl$_4$] (**3a**)

The compound [CpFe(CO)$_2${P(Cl)N-*i*-Pr$_2$}] (**1**) (100 mg, 0.291 mmol) was dissolved in CH_2Cl_2 (3 mL). Aluminium chloride (38.8 mg, 0.291 mmol) was then added, resulting in the formation of a red solution of **2a**. Diphenylacetylene (51.9 mg, 0.291 mmol) was added and the mixture was stirred for 15 min, resulting in a reddish orange solution. The solvent volume was reduced to ~0.5 mL. Pentane (10 mL) was added slowly with vigorous stirring, resulting in the formation of a yellow precipitate. The supernatant was decanted and the solid was washed with pentane (3 × 1 mL),

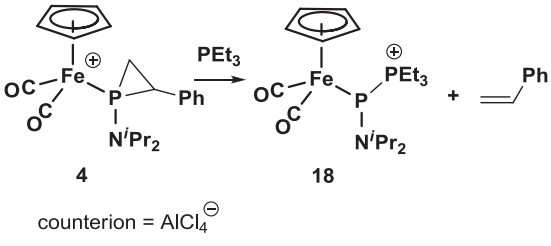

Scheme 11.

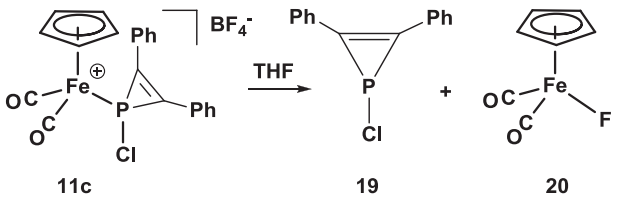

Scheme 12.

and dried under vacuum. Yield: 130 mg, 72%. IR (CH_2Cl_2 solution, cm^{-1}): νCO = 2059, 2016. ^1H NMR: δ 7.59–7.83 (m, Ph), 5.39 (d, 5H, $^3J(HP)$ = 1.5 Hz, C_5H_5), 3.57 (d sept, 2H, $^3J(HH)$ = 6.6 Hz, $^3J(HP)$ = 17.7 Hz, $CH(CH_3)_2$), 1.17 (d, 12H, $^3J(HH)$ = 6.6 Hz, $CH(CH_3)_2$). $^{31}P\{^1H\}$ NMR: δ −69.7 (s), ^{31}P NMR: δ −69.7 (t, $^3J(HP)$ = 17.7 Hz). ^{13}C NMR: δ 208.7 (d, $^2J(CP)$ = 31.9 Hz, $Fe(CO)_2$), 150.7 (d, $^1J(CP)$ = 13.1 Hz, phosphirene ring C), 130.3 (s, *p*-Ph), 130.4 (s, *m*-Ph), 129.4 (d, $^3J(CP)$ = 5.8 Hz, *o*-Ph), 127.1 (d, $^2J(CP)$ = 13.1 Hz, *ipso*-Ph), 87.4 (s, C_5H_5), 49.4 (d, $^2J(CP)$ = 4.3 Hz, $CH(CH_3)_2$), 23.4 (d, $^3J(CP)$ = 3.4 Hz, $CH(CH_3)_2$). MS (electrospray, CH_2Cl_2 solution): *m*/*z* = 486 (M^+). Anal. Calcd. For $C_{27}H_{29}O_2FePNAlCl_4$: C 49.50, H 4.46, N 2.14. Found: C 49.02, H 4.38, N 2.16.

4.2.2. [CpFe(CO)$_2${P(N-*i*-Pr$_2$)(C(Ph)C(Ph)}][BPh$_4$] (**3b**)

The compound [CpFe(CO)$_2${P(Cl)N-*i*-Pr$_2$}] (**1**) (50.0 mg, 0.146 mmol) was dissolved in CH_2Cl_2 (3 mL). This solution was added to sodium tetraphenylborate (49.8 mg, 0.146 mmol) and the mixture was stirred for 15 min. The resulting red solution of [CpFe(CO)$_2${PN-*i*-Pr$_2$}][BPh_4] (**2b**) was filtered through celite and added to PhCCPh (26.0 mg, 0.146 mmol). The mixture was stirred for 15 min, resulting in a reddish orange solution. The solvent volume was reduced to ~0.5 mL. The product was isolated as orange crystals by slow diffusion of pentane into the CH_2Cl_2 solution at −30 °C. Yield: 68 mg, 58%.

4.2.3. [CpFe(CO)$_2${P(N-*i*-Pr$_2$)(CH(Ph)CH$_2$)}][AlCl$_4$] (**4a**, **b**)

The compound [CpFe(CO)$_2${P(Cl)N-*i*-Pr$_2$}] (**1**) (50.0 mg, 0.146 mmol) was dissolved in CH_2Cl_2 (3 mL). This solution was added to $AlCl_3$ (29.0 mg, 0.217 mmol). To the resulting red solution of [CpFe(CO)$_2${PN-*i*-Pr$_2$}][$AlCl_4$] (**2a**) was added styrene (60.8 mg, 0.584 mmol, 67 μL) and the mixture was stirred for 15 min, resulting in a reddish orange solution. The solvent volume was reduced to ~0.5 mL. Addition of pentane (10 mL) resulted in a dark orange oil, which was washed with pentane and dried. Yield: 59 mg, 70%. Red-orange X-ray quality crystals were grown by slow diffusion of pentane into CH_2Cl_2 at −30 °C, and shown to contain **4a**, one of two diastereomers. IR (CH_2Cl_2 solution, cm^{-1}): νCO = 2074, 2032. $^{31}P\{^1H\}$ NMR: δ −52.0 (s) (81%), −53.8 (s) (19%). ^1H NMR (major diastereomer): δ 7.35–7.21 (m, Ph), 5.72 (s, C_5H_5), 3.59 (sept, $^3J(HH)$ = 6.9 Hz, $NCH(CH_3)_2$) 3.54 (sept, $^3J(HH)$ = 6.6 Hz, $NCH(CH_3)_2$), (s, $^3J(HH)$ = 2.72 (ddd, $^3J(HH)$ = 10.8 Hz, $^3J(HH)$ = 6.6 Hz, $^2J_{HP}$ = 10.8 Hz, CHPh), 2.01 (ddd, $^3J(HH)$ = 10.8 Hz, $^2J(HH)$ = 2.4 Hz, $^2J(HP)$ = 10.8 Hz, CHH), 1.56 (d, $^2J(HH)$ = 6.6 Hz, CHH), 1.38 (d, $^3J(HH)$ = 6.6 Hz, $NCH(CH_3)_2$), 1.37 (d, $^3J(HH)$ = 6.9 Hz, $NCH(CH_3)_2$). Satisfactory analysis could not be obtained because **4** exists in solution as an equilibrium mixture, and bulk samples always contain a proportion of **2**.

4.2.4. [CpFe(CO)$_2${P(N-*i*-Pr$_2$)(CH$_2$CHC(CH$_3$)CH$_2$)}][AlCl$_4$] (**6**)

Compound **1** (50.0 mg, 0.146 mmol) was dissolved in CH_2Cl_2 (3 mL). This solution was added to $AlCl_3$ (29.1 mg, 0.218 mmol). To the resulting red solution of [CpFe(CO)$_2${PN-*i*-Pr$_2$}][$AlCl_4$] (**2a**) was added isoprene (19.7 mg, 0.292 mmol, 29 μL) and the mixture was stirred for 1 h. The solvent volume was reduced to ~0.5 mL. Addition of pentane (10 mL) resulting in the formation of a brownish orange precipitate, which was washed with pentane and dried. Yield: 58 mg, 73%. IR (CH_2Cl_2 solution, cm^{-1}): νCO = 2073, 2035. ^1H NMR: δ 5.33 (br s, 5H, C_5H_5), 3.98 (dt, 1H, $^3J(HP)$ = $^3J(HH)$ = 6.9 Hz, −CH =), 3.69 (sept, 2H, $^3J(HH)$ = 6.9 Hz, $NCH(CH_3)_2$), 3.38 (m, 2H, $P(CH_2)CH$ =), 2.81 (bd, 1H, $^2J(HH_{gem})$ = 18.0 Hz, $PCHHC(CH_3)$), 2.81 (bd, 1H, $^2J(HH_{gem})$ = 18 Hz, $PCHHC(CH_3)$), 1.86 (s, 3H, CH_3), 1.31(d, 12H, $^3J(HH)$ = 6.9 Hz, $CH(CH_3)_2$). $^{31}P\{^1H\}$ NMR: δ 126.5 (s), ^{13}C NMR: δ 209.5 (d, $^2J(CP)$ = 24.6 Hz, Fe(CO)), 209.4 (d, $^2J(CP)$ = 24.8 Hz, Fe(CO)), 137.6 (d, $^2J(CP)$ = 8.7 Hz, =C(CH)$_3$), 121.3 (d, $^2J(CP)$ = 8.7 Hz, =CH), 87.8 (s, C_5H_5), 51.3 (d, $^2J(CP)$ = 3.4 Hz, $CH(CH_3)_2$), 46.2 (d, $^1J(CP)$ = 33.4 Hz, $P(CH_2)C(CH_3)$=), 42.8 (d, $^1J(CP)$ = 32.6 Hz, $P(CH_2)$ CH=), 23.8 (d, $^3J(CP)$ = 2.2 Hz, $CH(CH_3)_2$), 23.7 (d, $^3J(CP)$ = 2.2 Hz, $CH(CH_3)_2$, 16.3 (d, $^3J(CP)$ = 8.7 Hz, =C(CH_3)). MS (electrospray, CH_2Cl_2 solution): *m*/*z* = 376 (M^+). Compound **6** could not be crystallized and satisfactory analysis could not be obtained. As a result, the analogous compound **7** was prepared and fully characterized as described below.

4.2.5. [CpFe(CO)$_2${P(N-*i*-Pr$_2$)(CH(Ph)CH=CHCH(Ph))}][AlCl$_4$] (**7**)

The compound [CpFe(CO)$_2${P(Cl)N-*i*-Pr$_2$}] (**1**) (68.8 mg, 0.200 mmol) was dissolved in CH_2Cl_2 (3 mL). This solution was added to $AlCl_3$ (27.0 mg, 0.202 mmol). The resulting red solution of [CpFe(CO)$_2${PN-*i*-Pr$_2$}][$AlCl_4$] (**2a**) was transferred to a Schlenk flask equipped with a reflux condenser and then 1,4-diphenyl-1,3-butadiene (41.2 mg, 0.200 mmol) was added. The resulting solution was heated under reflux for 8 h. The mixture was allowed to cool to room temperature and the solvent volume was reduced to ~0.5 mL. Diethyl ether was added slowly with vigorous stirring, resulting in the formation of a brownish orange precipitate. The supernatant was decanted, and the solid was washed with diethyl ether (3 × 1 mL) and dried under vacuum. Crude yield: 81 mg, 59%. A portion of the precipitate (53.0 mg) was dissolved in CH_2Cl_2 (0.5 mL) and red-orange crystals were grown by slow diffusion of diethyl ether into the CH_2Cl_2 solution at − 30 °C. Overall yield: 31 mg, 35%. IR (CH_2Cl_2 solution, cm^{-1}): νCO = 2053, 2011. ^1H NMR: δ 7.17–7.40 (m, 10H, Ph), 6.23 (d, 2H, $^2J(HP)$ = 21.3 Hz, PCH(Ph)), 4.84 (d, 2H, $^3J(PH)$ = 11.1 Hz, =CH), 4.30 (s, 5H, C_5H_5), 3.89 (sept, 2H, $^3J(HH)$ = 6.9 Hz, $CH(CH_3)_2$), 1.48 (d, 12H, $^3J(HH)$ = 6.9 Hz, $CH(CH_3)_2$). $^{31}P\{^1H\}$ NMR: δ 175.2 (s). ^{13}C NMR: δ 209.0 (d, $^2J(CP)$ = 22.7 Hz, Fe(CO)$_2$), 137.7 (s, =CH), 133.3 (d, $^2J(CP)$ = 9.7 Hz, *ipso*-Ph), 130.1 (s, Ph), 129.8 (d, $^4J(CP)$ = 9.7 Hz, *m*-Ph), 129.2 (d, $^3J(CP)$ = 9.7 Hz, *o*-Ph), 87.3 (d, $^2J(CP)$ = 7.5 Hz, C_5H_5), 58.9 (br d, $^1J(CP)$ = 19.6 Hz, PC(Ph)), 52.5 (s, $CH(CH_3)_2$), 25.1 (s, $CH(CH_3)_2$). MS (electrospray, CH_2Cl_2 solution): *m*/*z* = 514 (M^+). Anal. Calcd. For $C_{29}H_{33}O_2FePNAlCl_4$: C 50.98, H 4.87, N 2.05. Found: C 50.16, H 4.89, N 2.08.

4.2.6. Synthesis of [CpFe(CO)$_2${P(N-*i*-Pr$_2$)(CH(Ph)CHC(CH$_3$)O)}][AlCl$_4$] (**8**)

The compound [CpFe(CO)$_2${P(Cl)N-*i*-Pr$_2$}] (**1**) (150 mg, 0.437 mmol) was dissolved in CH_2Cl_2 (3 mL). This solution was added to $AlCl_3$ (58.3.0 mg, 0.437 mmol). To the resulting red solution of [CpFe(CO)$_2${PN-*i*-Pr$_2$}][$AlCl_4$] (**2a**) was added benzylideneacetone (63.8 mg, 0.437 mmol) and the mixture was stirred for 15 min, resulting in a reddish orange solution. The solvent volume was reduced to ~0.5 mL and diethyl ether (10 mL) was added slowly with vigorous stirring, resulting in the formation of an orange precipitate. Crude yield: 245 mg, 90%. A portion of the precipitate (40.0 mg) was dissolved in CH_2Cl_2 (0.5 mL) and crystals were grown by slow diffusion of diethyl ether into the CH_2Cl_2 solution at −30 °C. Overall yield: 28 mg, 63%. IR (CH_2Cl_2 solution, cm^{-1}): νCO = 2058, 2016. ^1H NMR: δ 7.46–7.23 (m, 5H, Ph), 5.49 (broad d, 1H, $^2J(HP)$ = 27 Hz, =CH), 5.47 (s, 5H, C_5H_5), 4.32 (broad m, 1H, PCH), 3.53 (sept, 2H, $^3J(HH)$ = 6.6 Hz, $CH(CH_3)_2$), 2.15 (s, 3H,

CH_3), 1.06 (d, 6H, ^3J(HH) = 6.6 Hz, CH(CH_3)$_2$), 0.99 (d, 6H, ^3J(HH) = 6.6 Hz, CH(CH_3)$_2$). $^{31}P\{^1H\}$ NMR: δ 196.7 (s), ^{13}C NMR: δ 208.2 (d, ^2J(CP) = 27.6 Hz, Fe(CO)$_2$), 154.8 (s, POC), 134.2 (d, ^2J(CP) = 10.9 Hz, *ipso*-Ph), 126.9 (s, *o*-Ph), 128.7 (s, *m*-Ph), 128.6 (s, *p*-Ph), 104.8 (s, =CH), 86.0 (s, C_5H_5), 63.7 (d, ^1J(CP) = 21.7 Hz, PC(Ph)), 52.4 (d, ^2J(CP) = 5.8 Hz, $CH(CH_3)_2$), 25.3 (s, CH(CH_3)$_2$, 22.9 (d, ^3J(CP) = 5.6 Hz, CH(CH_3)$_2$, 16.3 (d, ^3J(CP) = 5.1 Hz, CH_3). MS (electrospray, CH_2Cl_2 solution): m/z = 454 (M^+). Anal. Calcd. For $C_{23}H_{29}O_3FePNAlCl_4$: C 44.34, H 4.69, N 2.25. Found: C 44.13, H 4.71, N 2.25.

4.2.7. Synthesis of [CpFe(CO)$_2${P(N-*i*-Pr$_2$)(PhNNHC$_6$H$_4$)}][AlCl$_4$] (**10**)

The compound [CpFe(CO)$_2${P(Cl)N-*i*-Pr$_2$}] (**1**) (175 mg, 0.509 mmol) was dissolved in CH_2Cl_2 (3 mL). This solution was added to $AlCl_3$ (69.0 mg, 0.510 mmol). The resulting red solution of [CpFe(CO)$_2${PN-*i*-Pr$_2$}][AlCl$_4$] (**2a**) was added to azobenzene (92.8 mg, 0.509 mmol) and the mixture was stirred for 1.5 h, resulting in a deep red solution. The solvent was removed under reduced pressure. The residue was washed with pentane (10 mL) to give brown-yellow powder. Yield: 190 mg, 57%. IR (CH_2Cl_2 solution, cm^{-1}): νCO = 2047, 2005. ^1H NMR: 7.86–7.06 (m, 9H, Ph, Ar), 7.39 (s, 1H, NH), 4.55 (d, 5H, ^3J(HP) = 1.5 Hz, C_5H_5), 3.55 (d sept, 2H, ^3J(HH) = 6.9 Hz, ^3J(HP) = 16.5 Hz, $CH(CH_3)_2$), 1.22 (d, 6H, ^3J(HH) = 6.6 Hz, CH(CH_3)$_2$), 1.03 (d, 6H, ^3J(HH) = 6.6 Hz, CH(CH_3)$_2$). $^{31}P\{^1H\}$ NMR: δ 117.5 (s). ^{13}C NMR: δ 209.2 (d, ^2J(CP) = 28.4 Hz, Fe(CO)$_2$), 208.6 (d, ^2J(CP) = 31.2 Hz, Fe(CO)$_2$), 143.9 (d, ^2J(CP) = 8.0 Hz, *ipso* Ph), 142.5 (d, ^2J(CP) = 10.0 Hz, Ar), 132.4 (s, Ar), 130.0 (s, Ar), 128.9 (s, Ph), 128.0 (s, Ph), 126.5 (d, ^1J(CP) = 16.5 Hz, *ipso* Ar), 123.5 (d, ^2J(CP) = 12.0 Hz, Ar), 123.3 (s, Ph), 121.8 (s, Ph), 117.7 (s, Ph), 114.1 (s, Ar), 87.2 (s, C_5H_5), 51.0 (d, ^2J(CP) = 6.6 Hz, $CH(CH_3)_2$), 22.6 (s, CH(CH_3)$_2$), 22.4 (s, CH(CH_3)$_2$). MS (electrospray, CH_2Cl_2 solution): m/z = 490 (M^+). Anal. Calcd. For $C_{25}H_{29}O_2N_3PFeAlCl_4$: C 45.56, H 4.43, N 6.38. Found: C 44.51, H 4.92, N 6.31.

4.3. P–N cleavage reactions

4.3.1. Reaction of [CpFe(CO)$_2${P(N-*i*-Pr$_2$)(C(Ph)C(Ph)}][AlCl$_4$] (**3a**) with HCl

Compound **3a** was prepared via reaction of **1** (82.0 mg, 0.239 mmol) with $AlCl_3$ (32.0 mg, 0.240 mmol) in CH_2Cl_2, followed by addition of diphenylacetylene (42.5 mg, 0.239 mmol). The mixture was stirred for 15 min, resulting in a reddish orange solution of **3a**. $HCl_{(g)}$ was then bubbled through the solution for 3 min. The flask was sealed and the solution was stirred for 15 h. The solvent volume was reduced to ~0.5 mL and diethyl ether (10 mL) was added slowly with vigorous stirring, resulting in the formation of a yellow precipitate, which contains [CpFe(CO)$_2${P(Cl)(C(Ph)C(Ph)}][AlCl$_4$] (**11a**) and the side product [H_2N-*i*-Pr$_2$]Cl. Crude yield: 96 mg. A portion of the crude precipitate (40 mg) was dissolved in ~1 mL of CH_2Cl_2 and filtered three times through a celite plug. Single crystals were grown by slow diffusion of hexane into the CH_2Cl_2 solution at − 30 °C. Yield: 61 mg, 45%. IR (CH_2Cl_2 solution, cm^{-1}): νCO = 2077, 2038. ^1H NMR: δ 7.93–7.73 (m, Ph), 4.89 (d, 5H, ^3J(HP) = 2.1 Hz, C_5H_5). $^{31}P\{^1H\}$ NMR: δ −52.0 (s), ^{13}C NMR: δ 206.3 (d, ^2J(CP) = 30.5 Hz, Fe(CO)$_2$), 144.5 (d, ^1J(CP) = 16.9 Hz, phosphirene ring C), 133.7 (s, *p*-Ph), 131.2 (d, ^2J(CP) = 7.2 Hz, *ipso*-Ph), 130.7 (s, *m*-Ph), 124.7 (s, *o*-Ph), 90.0 (s, C_5H_5). MS (electrospray, CH_2Cl_2 solution): m/z = 421(M^+, ^{35}Cl), 423 (M^+, ^{37}Cl).

4.3.2. Reaction of [CpFe(CO)$_2${P(N-*i*-Pr$_2$)(C(Ph)C(Ph)}][AlCl$_4$] (**3a**) with HBF$_4$·Et$_2$O

Compound **3a** (100 mg, 0.153 mmol) was dissolved in CH_2Cl_2 (2 mL) and $HBF_4\cdot Et_2O$ (73.8 mg, 0.459 mmol, 62.0 μL) was added. The resulting solution was stirred for 10 h. Diethyl ether (8 mL) was added, resulting in the formation of yellow precipitate, which contains [CpFe(CO)$_2${P(Cl)(C(Ph)C(Ph)}][BF$_4$] (**11c**) and the side product [H_2N-*i*-Pr$_2$][BF$_4$]. Crude yield: 74 mg. A portion of the crude precipitate (25 mg) was dissolved in CH_2Cl_2 (~1 mL) and filtered three times through a celite plug. Yellow crystals of **11c** were grown by slow diffusion of pentane into the CH_2Cl_2 solution at −30 °C. Yield: 6 mg, 33%. Anal. Calcd. For $C_{21}H_{15}O_2FePClBF_4$: C 49.61, H 2.97. Found: C 49.86, H 2.89. Spectroscopic data for **11c** is identical to that of **11a**.

4.3.3. Synthesis of [CpFe(CO)$_2${P(Cl)(PhNNHC$_6$H$_4$)}][(AlCl$_4$)$_{0.5}$(BF$_4$)$_{0.5}$] (**12**)

Compound **7** (40.0 mg, 0.061 mmol) was dissolved in CH_2Cl_2 (2 mL), $HBF_4\cdot Et_2O$ (29.8 mg, 25.0 μL, 0.184 mmol) was added, and the resulting solution was stirred for 2 h. The solvent volume was reduced to ~0.2 mL and it was cooled −30 °C, resulting in the formation of orange crystals. Yield: 17 mg, 55%. IR (CH_2Cl_2 solution, cm^{-1}): νCO = 2074, 2037. ^1H NMR (DMSO): δ 7.88–7.60 (m, 9H, Ph, Ar), 7.59 (s, 1H, NH), 5.34 (d, 5H, ^3J(HP) = 2.1 Hz, C_5H_5). $^{31}P\{^1H\}$ NMR (DMSO): δ 144.4 (s). ^{13}C NMR (DMSO): δ 210.9 (d, ^2J(CP) = 32.8 Hz, Fe(CO)$_2$), 152.8 (s, *ipso*-Ph), 151.6 (d, ^2J(CP) = 7.2 Hz, Ar), 141.3 (s, Ar), 140.5 (s, Ar), 133.6 (s, Ar), 132.5 (s, *p*-Ph), 131.8 (d, ^2J(CP) = 9.4 Hz, *ipso*-Ar), 131.6 (d, ^2J(CP) = 9.4 Hz, Ar), 130.1 (s, *m*-Ph), 123.6 (s, *o*-Ph), 88.5 (s, C_5H_5). MS (electrospray, CH_2Cl_2 solution): m/z = 425 (M^+, ^{35}Cl), 427 (M^+, ^{37}Cl). Anal. Calcd. For $C_{19}H_{15}O_2FePN_2Cl_3Al_{0.5}B_{0.5}F_2$: C 42.69, H 2.83. Found: C 42.64, H 3.11. Note: The presence of mixed $AlCl_4^-/BF_4^-$ counterions in the crystals was confirmed by ^{19}F NMR and negative ion electrospray MS.

4.3.4. Reaction of [CpFe(CO)$_2${P(N-*i*-Pr$_2$)(CH(Ph)CH$_2$)}][AlCl$_4$] (**4**) with HCl

The compound [CpFe(CO)$_2${P(Cl)N-*i*-Pr$_2$}] (**1**) (30.0 mg, 0.087 mmol) was dissolved in CH_2Cl_2 (3 mL). This solution was added to $AlCl_3$ (17.4 mg, 0.131 mmol). To the resulting red solution of [CpFe(CO)$_2${PN-*i*-Pr$_2$}][AlCl$_4$] (**2a**) was added styrene (36.2 mg, 0.348 mmol, 40.0 μL)) and the mixture was stirred for 15 min, resulting in a reddish orange solution of **4**. Hydrogen chloride gas was bubbled through CH_2Cl_2 (3 mL) and the resulting solution was transferred via cannula into the solution of **4**. After 30 min the volume of the solvent was reduced to ~0.5 mL under reduced pressure and transferred into a NMR tube. Yellow crystals of [CpFe(CO)$_2${PH(N-*i*-Pr$_2$)(Cl)}][AlCl$_4$] (**13**) were obtained by slow diffusion of pentane into CH_2Cl_2 solution. Yield: 26 mg, 58%. IR (CH_2Cl_2 solution, cm^{-1}): νCO = 2073, 2035. ^1H NMR: δ 8.79 (d, 1H, ^1J(PH) = 471 Hz, P*H*), 5.49 (d, 5H, ^3J(HP) = 2.1 Hz, C_5H_5), 3.81 (dsept, 2H, ^3J(PH) = 14.8 Hz, ^3J(HH) = 6.6 Hz, $CH(CH_3)$), 1.46 (d, 6H, ^3J(HH) = 6.6 Hz, CH(CH_3)), 1.35 (d, 6H, ^3J(HH) = 6.6 Hz, CH(CH_3)). $^{31}P\{^1H\}$ NMR: δ 106.4 (s), ^{31}P NMR: δ 106.4 (dt, ^1J(PH) = 471 Hz, ^3J(PH) = 14.8 Hz). MS (electrospray, CH_2Cl_2 solution): m/z = 344 (M^+, ^{35}Cl), 346 (M^+, ^{37}Cl). Anal. Calcd. For $C_{13}H_{20}O_2FePNAlCl_5$: C 30.42, H 3.93, N 2.73. Found: C 30.45, H 3.85, N 2.62.

4.4. Decomplexation reactions

4.4.1. Decomplexation of [CpFe(CO)$_2${P(N-*i*-Pr$_2$)(C(Ph)C(Ph)}][AlCl$_4$] (**3a**)

Compound **3a** (225 mg, 0.328 mmol) was dissolved in CH_2Cl_2. Trimethylphosphine (49.9 mg, 0.656 mmol, 67.3 μL) was added and the solution was stirred for 2 h. The solvent was removed under reduced pressure, and the residue was extracted into pentane (5 × 3 mL). The solvent volume was reduced to ~1 mL under reduced pressure and the pentane extract was cooled to −30 °C for 48 h, resulting in the formation of pale yellow crystals of PN-*i*-Pr$_2$(C(Ph)C(Ph)) (**15**). The pentane insoluble residue was extracted into CH_2Cl_2 (1 mL). Pentane (10 mL) was added slowly with mixing, resulting in the formation of a yellow orange precipitate of

[CpFe(CO)$_2${P(PMe$_3$)}][AlCl$_4$] (**14**). The supernatant was decanted and solid was dried under reduced pressure. The counterion AlCl$_4$ was exchanged with BPh$_4$ to grow single crystals. The solid **14** (43.0 mg, 0.100 mmol) and NaBPh$_4$ (34.2 mg, 0.100 mmol) were dissolved in CH$_2$Cl$_2$ (2 mL) and the resulting solution was stirred for 30 min. The precipitate formed was removed by filtration to form a clear solution of [CpFe(CO)$_2${P(CH$_3$)$_3$}][BPh$_4$]. Single crystals were grown by slow diffusion of hexane into the CH$_2$Cl$_2$ solution at −30 °C. Compound **14**: Yield: 102 mg, 64%. IR (CH$_2$Cl$_2$ solution, cm^{-1}): νCO = 2052, 2010. ^{1}H NMR: δ 5.42 (d, 5H, ^{3}J(HP) = 1.5 Hz, C$_5$*H*$_5$), 1.82 (d, 9H, ^{2}J(PH) = 11.1 Hz, PC*H*$_3$). ^{31}P{^{1}H} NMR: δ 33.5 (s), ^{31}P NMR: δ 33.5 (dec., ^{2}J(PH) = 11.1 Hz). MS (electrospray, CH$_2$Cl$_2$ solution): *m*/*z* = 253 (M$^+$). Compound **15**: Yield: 38 mg, 37%. ^{1}H NMR: δ 7.33–7.81 (m, 10H, Ph), 3.16 (d sept, ^{3}J(PH) = 8.7 Hz, ^{3}J(HH) = 6.6 Hz, C*H*(CH$_3$)$_2$), 1.10 (d, ^{3}J(HH) = 6.6 Hz, CH(C*H*$_3$)$_2$). ^{31}P{^{1}H} NMR: δ −125.1 (s). ^{13}C NMR: δ 136.0 (d, ^{1}J(CP) = 53.7 Hz, phosphirene ring C), 131.9 (d, ^{2}J(CP) = 5.8 Hz, *ipso*-Ph), 130.4 (s, *o*-Ph), 129.6 (s, *m*-Ph), 128.6 (s, *p*-Ph), 43.9 (d, ^{2}J(CP) = 6.6 Hz, *C*H(CH$_3$)$_2$), 23.8 (d, ^{3}J(CP) = 8.0 Hz, CH(*C*H$_3$)$_2$). Anal. Calcd. For C$_{20}$H$_{24}$PN: C 77.64, H 7.82, N 4.53. Found: C 77.64, H 7.81, N 4.57.

4.4.2. Decomplexation of [CpFe(CO)$_2${P(N-*i*-Pr$_2$)(CH(Ph)CHCHCH(Ph))}][AlCl$_4$] (**7**)

Compound **7** was (112 mg, 0.164 mmol) dissolved in CH$_2$Cl$_2$. Triethylphosphine (38.8 mg, 0.328 mmol, 48 μL) was added and the resulting solution was refluxed for 10 h. The solvent was removed under reduced pressure and the product was extracted in pentane (10 mL). Pentane was removed under reduced pressure and pale yellow solid P(N-*i*-Pr$_2$)(CH(Ph)CHCHCH(Ph)) (**16**) was obtained. Yield: 31 mg, 56%. ^{1}H NMR: δ 7.17–7.40 (m, Ph), 5.89 (d, ^{2}J(HP) = 8.1 Hz, PC*H*(Ph)), 4.11 (d, ^{3}J(PH) = 5.7 Hz, −C*H* =), 3.45 (b, C*H*(CH$_3$)$_2$), 0.98 (d, ^{3}J(HH) = 6.6 Hz, CH(C*H*$_3$)$_2$). ^{31}P{^{1}H} NMR: δ 91.4 (s). ^{13}C NMR: δ 144.0 (d, ^{2}J(CP) = 15.4 Hz, =*C*H), 133.6 (d, ^{2}J(CP) = 11.0 Hz, *ipso*-Ph), 128.5 (d, ^{5}J(CP) = 2.2 Hz Ph), 127.7 (d, ^{4}J(CP) = 6.6 Hz, *m*-Ph), 125.8 (d, ^{3}J(CP) = 2.9 Hz, *o*-Ph), 51.2 (d, ^{2}J(CP) = 19.2 Hz, *C*H(CH$_3$)$_2$), 46.9 (br, PC(Ph)), 24.2 (d, ^{3}J(CP) = 5.9 Hz, CH(*C*H$_3$)$_2$).

4.4.3. Decomplexation of [CpFe(CO)$_2${P(N-*i*-Pr$_2$)(CH(Ph)CHC(CH$_3$)O)}][AlCl$_4$] (**8**)

Compound **8** (245 mg, 0.393 mmol) was dissolved in CH$_2$Cl$_2$ (5 mL) and transferred to a Schlenk flask. Trimethylphosphine (44.8 mg, 0.590 mmol, 61.0 μL) was added and the resulting solution was stirred for 1 h. The solvent was removed under reduced pressure and the product was extracted in pentane (10 mL). Pentane was removed under reduced pressure and P(N-*i*-Pr$_2$)(CH(Ph)CHC(CH$_3$)O) (**17**) was obtained as a colourless oil. Yield: 53 mg, 47%. ^{1}H NMR: δ 7.05–7.22 (m, Ph), 5.04 (ddq, 1H, ^{3}J(PH) = 10.2 Hz, ^{3}J(HH) = 0.9 Hz, ^{4}J(HH) = 1.8 Hz, =C*H*), 4.33 (br d, 1H, ^{2}J(PH) = 32.1 Hz, PC(Ph)*H*), 3.00 (b, 2H, C*H*(CH$_3$)$_2$), 1.90 (d, 3H, ^{4}J(HH) = 1.6 Hz, C*H*$_3$), 1.11 (b, 12H, C*H*$_3$). ^{31}P{^{1}H} NMR: δ 137 (s). ^{13}C NMR: δ 156.6 (d, ^{2}J(CP) = 11.5 Hz, =*C*(Me)O), 130.9 (d, ^{2}J(CP) = 8.8 Hz, *ipso*-Ph), 128.2 (s, Ph), 125.5 (s, Ph), 97.8 (s, =*C*H), 50.2 (d, ^{1}J(CP) = 28.2 Hz, P*C*H(Ph)), 29.9 (s, *C*H(CH$_3$)$_2$), 24.7 (s, *C*H$_3$), 16.6 (s, CH(*C*H$_3$)$_2$).

4.4.4. Reaction of [CpFe(CO)$_2${P(N-*i*-Pr$_2$)(CH(Ph)CH$_2$)}][AlCl$_4$] with PEt$_3$ (**4**)

Compound **4** was prepared from **1** (40.0 mg, 0.116 mmol), AlCl$_3$ (15.6 mg, 0.116 mmol) and styrene (48.4 mg, 0.464 mmol, 53.0 μL). Triethylphosphine (13.7 mg, 0.116 mmol, 17.0 μL) was added and the resulting mixture was stirred for 15 min. The solvent volume was reduced to ~0.5 mL. Pentane (10 mL) was added slowly with vigorous stirring, resulting in the formation of an orange precipitate. Yield: 40.7 mg, 59%. Orange crystals of [CpFe(CO)$_2${P(N-*i*-Pr$_2$)(PEt$_3$)}][AlCl$_4$] (**18**) were obtained by slow diffusion of hexane into CH$_2$Cl$_2$ solution. Yield: 35 mg, 51%. IR (CH$_2$Cl$_2$ solution, cm^{-1}): νCO = 2048, 2000. ^{1}H NMR: δ 5.16 (d, 5H, ^{3}J(HP) = 2.7 Hz, C$_5$*H*$_5$), 3.27 (br, 2H, C*H*(CH$_3$)), 2.12 (dq, 6H, ^{2}J(PH) = 10.0 Hz, ^{3}J(HH) = 7.6 Hz, PC*H*$_2$CH$_3$), 1.33 (d *t*, 9H, ^{3}J(PH) = 15.8 Hz, ^{3}J(HH) = 7.6 Hz, PCH$_2$C*H*$_3$), 1.17 (d, 12H, ^{3}J(HH) = 6.6 Hz, CH(C*H*$_3$)). ^{31}P NMR: δ 84.6 (br d, ^{1}J(PP) = 514 Hz, Fe*P*P), 33.4 (br d ^{1}J(PP) = 514 Hz, FeP*P*). Anal. calcd. for C$_{19}$H$_{34}$O$_2$FeP$_2$NAlCl$_4$: C 38.35, H 5.76, N 2.35. Found: C 38.41, H 5.45, N 2.26.

4.4.5. Decomplexation of [CpFe(CO)$_2${P(Cl)(C(Ph)C(Ph)}][BF$_4$] (**11c**)

Compound **11c** (191 mg, 0.376 mmol) was dissolved in THF and stirred for 30 min. The THF was removed under reduced pressure and the residue was dissolved in CH$_2$Cl$_2$. Column chromatography (silica gel, CH$_2$Cl$_2$ eluent) was used to isolate two fractions, one colourless and one orange. The solvent was removed under reduced pressure and the products were dissolved in pentane (1 mL). The pentane extracts were cooled to −30 °C for 60 h, resulting in the formation of white crystals of PCl(C(Ph)C(Ph)) (**19**) and orange crystals of [CpFe(CO)$_2$PF] (**20**). Compound **19**: Yield: 28 mg, 46%. ^{1}H NMR: δ 7.52–7.99 (m, Ph). ^{31}P{^{1}H} NMR: δ −80.7 (s). ^{13}C NMR: δ 134.7 (d, ^{1}J(CP) = 65.5, phosphirene C), 129.9 (s, *C*-Ph), 128.2 (s, *C*-Ph), 126.4 (d, ^{2}J(CP) = 8.8 Hz, *ipso*-Ph). Compound **20**: Yield: 47 mg, 87%. IR (CH$_2$Cl$_2$ solution, cm^{-1}): νCO = 2057, 2012. ^{1}H NMR: δ 4.98 (s, C$_5$*H*$_5$). ^{19}F{^{1}H} NMR: δ −149.2 (s).

4.5. X-ray crystallography

Suitable crystals of compounds **3b**, **4a**, **7**, **8**, **10**, and **14** were mounted on glass fibres. Programs for diffractometer operation, data collection, cell indexing, data reduction and absorption correction were those supplied by Bruker AXS Inc., Madison, WI. Diffraction measurements were made on a PLATFORM diffractometer/SMART 1000 CCD using graphite-monochromated Mo-Kα radiation at −80 °C. The unit cell was determined from randomly selected reflections obtained using the *SMART CCD* automatic search, centre, index and least-squares routines. Integration was carried out using the program *SAINT* and an absorption correction was performed using *SADABS*. Structure solution was carried out using the *SHELX97* [36] suite of programs and the *WinGX* graphical interface [37]. Initial solutions were obtained by direct methods and refined by successive least-squares cycles. All non-hydrogen atoms were refined anisotropically.

Acknowledgements

This work was financially supported by the University of Regina. We also thank Bob McDonald and Mike Ferguson (University of Alberta) for X-ray data collection.

Appendix A. Supplementary material

CCDC 945774, 945775, 945776, 945777, 945778 and 945779 contain the supplementary crystallographic data for this paper. These data can be obtained free of charge from The Cambridge Crystallographic Data Centre via www.ccdc.cam.ac.uk/data_request/cif.

References

[1] G. Frison, F. Mathey, A. Sevin, J. Organomet. Chem. 570 (1998) 225–234.
[2] A.W. Ehlers, E.J. Baerends, K. Lammertsma, J. Am. Chem. Soc. 124 (2002) 2831–2838.
[3] H. Aktaş, J. Slootweg, K. Lammertsma, Angew. Chem. Int. Ed. 49 (2010) 2102–2113.
[4] A. Marinetti, F. Mathey, J. Am. Chem. Soc. 104 (1982) 4484–4485.

[5] F. Mathey, N.H. Tran Huy, A. Marinetti, Helv. Chim. Acta 84 (2001) 2938–2957.
[6] K. Lammertsma, M.J.M. Vlaar, Eur. J. Org. Chem. (2002) 1127–1138.
[7] F. Mathey, Dalton Trans. (2007) 1861–1868.
[8] A.W. Ehlers, K. Lammertsma, E.J. Baerends, Organometallics 17 (1998) 2738–2742.
[9] S. Creve, K. Pierloot, M.T. Nguyen, L.G. Vanquickenborne, Eur. J. Inorg. Chem. (1999) 107–115.
[10] K.K. Pandey, A. Lledós, J. Organomet. Chem. 695 (2010) 206–214.
[11] K.K. Pandey, P. Tiwari, P. Patidar, J. Phys. Chem. A 116 (2012) 11753–11762.
[12] B.T. Sterenberg, K.A. Udachin, A.J. Carty, Organometallics 20 (2001) 2657–2659.
[13] J. Sánchez-Nieves, B.T. Sterenberg, K.A. Udachin, A.J. Carty, J. Am. Chem. Soc. 125 (2003) 2404–2405.
[14] B.T. Sterenberg, K.A. Udachin, A.J. Carty, Organometallics 22 (2003) 3927–3932.
[15] T.W. Graham, K.A. Udachin, A.J. Carty, Chem. Commun. (2005) 5890–5892.
[16] T.W. Graham, R.P.Y. Cariou, J. Sanchez-Nieves, A.E. Allen, K.A. Udachin, R. Regragui, A.J. Carty, Organometallics 24 (2005) 2023–2036.
[17] B.T. Sterenberg, O.S. Senturk, K.A. Udachin, A.J. Carty, Organometallics 26 (2007) 925–937.
[18] K. Vaheesar, T.M. Bolton, A.L.L. East, B.T. Sterenberg, Organometallics 29 (2010) 484–490.
[19] F. Mathey, Chem. Rev. 90 (1990) 997–1025.
[20] M. Baudler, Angew. Chem. Int. Ed. 21 (1982) 492–512.
[21] M. Baudler, Pure Appl. Chem. 52 (1980) 755–769.
[22] S.S. Al-Juaid, D. Carmichael, P.B. Hitchcock, S. Lochschmidt, A. Marinetti, F. Mathey, J.F. Nixon, J. Chem. Soc. Chem. Commun. (1988) 1156–1158.
[23] T.W. Graham, K.A. Udachin, M.Z. Zgierski, A.J. Carty, Organometallics 30 (2011) 1382–1388.
[24] A. Marinetti, F. Mathey, Organometallics 3 (1984) 456–461.
[25] H.T.H. Ngoc, L. Ricard, F. Mathey, New J. Chem. 22 (1998) 75–76.
[26] A. Davison, M.L.H. Green, G. Wilkinson, J. Chem. Soc. (1961) 3172–3177.
[27] T.I. Kückmann, F. Dornhaus, M. Bolte, H.-W. Lerner, M.C. Holthausen, M. Wagner, Eur. J. Inorg. Chem. (2007) 1989–2003.
[28] W.F. McNamara, H.U. Reisacher, E.N. Duesler, R.T. Paine, Organometallics 7 (1988) 1313–1317.
[29] W. Schnurr, M. Regitz, Tetrahedron Lett. 30 (1989) 3951–3954.
[30] W. Malisch, P. Panster, J. Organomet. Chem. 64 (1974) C5–C9.
[31] A. Hildebrand, I. Sarosi, P. Lonnecke, L. Silaghi-Dumitrescu, M.B. Sarosi, I. Silaghi-Dumitrescu, E. Hey-Hawkins, Dalton Trans. 41 (2012) 7729–7736.
[32] H. Hacklin, G.-V. Röschenthaler, Phosphorus, Sulfur Silicon Relat. Elem. 36 (1988) 165–169.
[33] M. Gerdin, M.l. Penhoat, R. Zalubovskis, C. Pétermann, C. Moberg, J. Organomet. Chem. 693 (2008) 3519–3526.
[34] A. Tarasevych, A. Rozhenko, G.-V. Röschenthaler, I. Shevchenko, Phosphorus Sulfur Silicon Relat. Elem. 186 (2011) 841–844.
[35] K. Junge, G. Oehme, A. Monsees, T. Riermeier, U. Dingerdissen, M. Beller, J. Organomet. Chem. 675 (2003) 91–96.
[36] G.M. Sheldrick, SHELX97-Programs for Crystal Structure Analysis, 1998.
[37] L.J. Farrugia, J. Appl. Cryst. 32 (1999) 837–838.